Received: 23 August 2015

Preliminary stock assessment of blue shark (*Prionace glauca*) caught in the Indian Ocean using a Bayesian state-space production model

Andrade, H. A.

Federal Rural University of Pernambuco (UFRPE)
Department of Fisheries and Aquaculture (DEPAq)
Applied Statistics Modeling (MOE)

Abstract

Bayesian state-space models were fitted to four standardized catch rates of blue shark (*Prionace glauca*) caught in the Indian Ocean. Estimations of catches as reported in the IOTC databases were the base case, though alternative estimation of catches was considered in the sensitivity analyses. Uncertain is high as indicated by the wide posteriors of parameters. The preliminary estimations showed in this paper indicate that biomassa of blue shark population is above the biomass at MSY, but the harvest rate is close or above the harvest hat at MSY.

Introduction

Blue shark (BSH) (*Prionace glauca*) is a cosmopolitan species which has been caught all around the world by fleets which operate different types of gears. Catches of blue are often higher than catches of other elasmobranch, or even higher than catches of some species of teleosts. In the Indian Ocean most of the blue shark has been caught by India, Spain, Japan, Taiwan and Portugal as reported in the Indian Ocean Tuna Commission (IOTC) databases (IOTC, 2015). The majority of fish was caught by boats of India which operates lines and gillnets, while Spanish, Japanese, Taiwanese and Portuguese fishermen catches blue shark when operating longlines aiming at tunas or swordfish.

In spite the fairly high catches stock assessment of Indian Ocean blue shark were not carrying previous years. However, there is enough information to run stock assessment models. Surplus production models demand catch and relative abundance indices (or effort). Recently the catch-per-unit-effort (CPUE) time series of Japan, Portugal, Spain and Taiwan fleets were standardized in an attempt to estimate relative abundance indices (Coelho et al., 2014; Coelho et al., 2015; Fernández-Costa et al., 2015; Tsai and Liu, 2014). In addition there is the catch times series estimated by the IOTC (IOTC, 2015), and there are estimations calculated using models based on alternative indicators (e.g. fin market) (Clarke, 2015). All the available catch and standardized CPUE times were used in this paper to assess the blue shark population of Indian Ocean using a state-space Bayesian production model (SBPM).

2. Data

There is one catch time series estimated by the IOTC (IOTC, 2015), and five alternative catch time series estimated using alternative approaches (Clarke, 2015) (Figure 2 A). The main difference is the scale, IOTC estimations reaches 30 thousand tons while the alternative estimations reaches close to 250 thousand tons. In spite of the huge differences concerning the values, all of the catch estimations had increased across the years in similar proportional pace. In this paper, the catch of IOTC is the base case, while the longest alternative time series was considered in a sensitivity analysis.

Estimations of standardized CPUE of Japan, Portugal (Coelho et al., 2014) and Taiwan (Tsai and Liu, 2014) were presented in the 10th Working Party on Ecosystems and Bycatch (WPBEB10) hold in 2014. This year estimations of standardized CPUE of Spain were provided by Fernández-Costa et al. (2015), and the estimation of standardized cpue of Portugal was updated (Coelho et al., 2015).

All the series were scaled by dividing the values by the mean to make comparisons easier (Figure 2 B). Notice that some of the series showed peaks (e.g. JPN and TWN), while the others showed smoothed time trends, specially the series of Spain. Notice also the series of Portugal showed a steady decreasing trend.

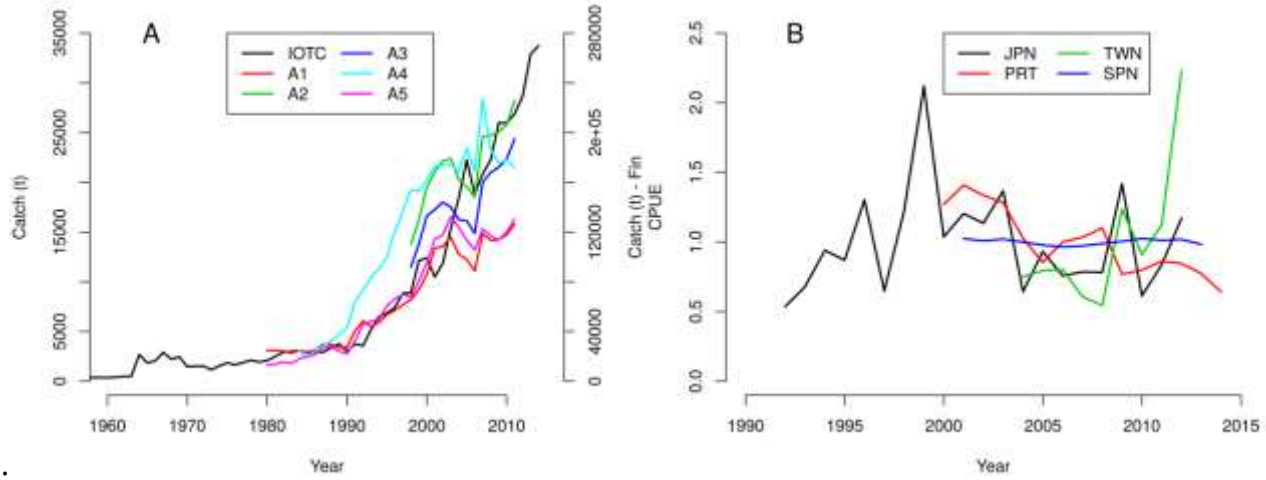

.

Figure 1 – Estimations of catches (A) and catches-per-unit-effort (CPUE) (B) used in the analyses. IOTC – estimation as reported in IOTC database; A1 – A5 – estimations of catches based on alternative approaches (see Clarke, 2015). JPN- Japan, PRT – Portugal, TWN – Taiwan, and SPN – Spain.

3. Model

The model used here is fully described in the paper of Meyer and Millar (1999). The model was already used before in the some IOTC meetings (e.g. Working Parties on Billfish 11 and 12). Applications in stock assessment of bycatch species caught in longline fisheries targeting tuna and tuna like species in Indian Ocean can be found in (Andrade, 2013 and 2014). However the model was adapted to allow using multiple CPUE time series as calculated based on different fleets. Here follows a summary of the model version used in this paper, and also the description of the calculation procedures. The observed data are represented by vectors with values for yields and abundance indices denoted by $Y_t$and I_t, respectively, where $t = 1, \dots, N$ is the index for the year. The general biomass dynamic equation is:

$$B_t = B_{t-1} + g(B_{t-1}) - Y_{t-1} \quad (1)$$

Where B_t is the biomass at the beginning of year t, Y_t is the yield obtained during this year (all fleets aggregated), and $g(\ )$is the "surplus production" function. The formulae of Schaefer $g(B_{t-1}) = rB_{t-1}(1 - B_{t-1}/k)$ is often used here, where k is the carrying capacity and r is the intrinsic growth rate of the population.

It is assumed the link between the unobserved state (B_t) and the observed abundance indices in the t^{th} year (I_{tm}) can be represented by the equation:

$$I_{tm} = q_m B_t \quad (2)$$

where q_m is the catchability coefficient of the m^{th} fleet. Management reference points may be calculated based on the estimations of the parameters r, k and eventually q_m.

These calculations can be considered in the context of a state-space model which includes process and observational uncertainties. In this case, the observed series of data (I_t) is linked to the

unobserved states (B_t) through a stochastic model. This version of the model is reparametrized by the calculation of the proportion of the annual biomass in relation to the carrying capacity ($P_t = B_t/k$), which results in an improvement in the performance of the Gibbs sampler (MCMC) used in the Bayesian approach to generate the sample of the posterior distribution. The state equations may thus be written in the stochastic form, as:

$$P_1 |\sigma^2 = e^{u_1} \qquad (3)$$
$$P_t|P_{t-1}, k, r, \sigma^2 = [P_{t-1} + g(P_{t-1}) - Y_{t-1}/k]e^{u_t} t = 2, \dots, N$$

while the equations for the observations would be:

$$I_{tm}|P_t, q_m, \tau^2 = q_m k P_t e^{v_t} t = 2, \dots, N \qquad (4)$$

Where $u_t$is an independent and identically distributed (*iid*) normal random variable with mean 0 and variance σ^2, while v_t is a normal *iid* with mean 0 and variance τ^2. Lognormal models were thus used for both observational and process equations.

If independent priors are assumed for the three parameters (k, r, q) of the biomass dynamic model and those that describe the errors (σ^2, τ^2), the prior distribution of these parameters and of the states ($P_1, \dots, P_N$) is:

$$p(k, r, q_1, \dots, q_m, \sigma^2, \tau^2, P_1, \dots, P_n) =$$
$$p(k)p(r)p(q_1) \dots p(q_m)p(\sigma^2)p(\tau^2)p(P_1|\sigma^2) \prod_{i=2}^{N} p(P_t|P_{t-1}, k, r, \sigma^2) \qquad (5)$$

The joint sample distribution for the abundance indices is given by:

$$p(I_1, \dots, I_N|k, r, q, \sigma^2, \tau^2, P_1, \dots, P_N) = \prod_{t=1}^{N} p(I_t|P_t, q, \tau^2) \qquad (6)$$

and finally, the posterior distribution for the parameters, states, and observations is:

$$p(k, r, q, \sigma^2, \tau^2, P_1, \dots, P_N, I_1, \dots, I_N) =$$
$$p(k)p(r)p(q)p(\sigma^2)p(\tau^2)p(P_1|\sigma^2) \prod_{t=2}^{N} p(P_t|P_{t-1}, k, r, \sigma^2) \prod_{t=1}^{N} p(I_t|P_t, q, \tau^2) \qquad (7)$$

Numerical Monte Carlo procedures can be used to obtain a sample of the joint posterior distribution. In the present study, a Markov Chain Monte Carlo (MCMC) algorithm was used, and the Gibbs sampler was implemented in the JAGS program (Plummer, 2005) available in the R program (R Core Team 2014) with the *runjags* package (Denwood, 2009). Three chains were initiated with different initial values for the parameters. The first 30,000 values of each chain were eliminated as burnin, and values were retrieved at every 30 steps (slice sampling) of the subsequent 90000 steps of the chain, providing a set of 3000 values of the posterior distribution for each chain.

4. Priors

Informative or non-informative priors can be used here, depending on the availability of information and knowledge on the species and the stock being analyzed, or even similar species or stocks (McAllister and Kirkwood,1998, McAllister et al.,1994, Punt and Hilborn, 1997). Both non-informative and informative prior models were fitted in order to assess the effect of the prior assumptions. Jeffrey's non-informative reference prior for $q$is independent of r and k, and is equivalent to a uniform prior on a logarithmic scale (Millar, 2002). Therefore, the wide uniform prior $U(-45, -1)$ on the logarithmic scale was used in the present study for the catchabilities of all fleets $q_1, \dots, q_m$. For r and k, wide uniform priors that convey little information on the parameters were used. The uniform prior for k with lower and upper limits defined in tons was $U(35000{,}20 \times$

50000). The lower limit is close to the maximum annual yield as reported in IOTC database. The prior for r was $U(0,2)$, and those for $\sigma^2$and τ^2were the inverse gamma $IG(1,0.1)$and $IG(1,0.1)$, respectively.

This year Atlantic blue shark stocks were assessed and the informative priors previously used were updated in the light of the new biological information (Anon, 2015). Lognormal prior with mean of 0.22 and low standard deviation of 0.072 (Carvalho and Winker, 2015) or median close to 0.32 and low standard deviation of 0.043 (Babcock and Cortés, 2015) were used for the r. In this paper the tentative informative prior for r was a lognormal with mean 0.3 but I have, but with a standard deviation of 0.3 which is fairly high for an informative prior. The decision of not using a very restrictive prior for Indian Ocean was because this is the very first attempt to assess the blue shark of Indian Ocean. It seems reasonable to start by discussing the available biological information before building very informative and restrictive priors. In this sense, the calculations showed in this papers stand as a preliminary approach. Same rationale underpins the tentative informative prior for k used here. It was used a lognormal with mean of 300,000 t but with a fairly high standard deviation and bounded at 700,000 t. This prior gives weight to the hypothesis that the carrying capacity of all Indian Ocean is fairly higher than the sum of carrying capacities of the North and South Atlantic aggregated (Anon, 2015). The intention was to not restrict much the upper limit of the posteriors in this preliminary analysis. However, like mentioned above when showing the prior of r, the informative prior of k for Indian Ocean also demands further discussion. I did not found sound information about the other parameters of the models (i.e. q), hence no informative prior was used.

5. Diagnostics and Convergence

Graphs (e.g. traceplots) and diagnostic tests were used to determine whether a stationary distribution had been reached. These analyses were run in the CODA library (Plummer et al., 2006). Gelman and Rubin's (1992) statistic was used for diagnosis. Convergence was assumed when the 97.5% quantile of the Potential Scale Reduction Factor (PSRF) was equal to or lower than 1.05. Autocorrelations were also used to evaluate the mixing degree of the samples of the posterior distribution. Estimations of the some parameters are usually correlated, hence coefficient of correlations were calculated and the joint posterior were examined. Residuals were also investigated to assess the quality of the fittings to each time series.

6. Results

Catch and catch rates

Distributions of frequencies, relationships and coefficients of correlations of available estimations of catches and catch rates available are showed in Figure 2. The correlations of catches with year were all positive, as well as the correlations between catch estimations. All the catch time series are in agreement in the sense they all showed that catches had increased across the years in similar pace.

Correlations between year and catch rates of Japan and of Spain were very low. However the correlations between year and catch rates of the other fleets were strongly negative (Portugal), or positive (Taiwan). These results indicate that time series are conflictive, particularly those estimated for Portugal and for Taiwan. That conclusion also arises if we consider the negative coefficient of correlation between catch rates of Portugal and Taiwan. Notice also that catch rate of Portugal is the negatively correlated with all the catch estimations. Both positive and negative correlations appear when comparing the catches series to the catch rates estimated for other fleets.

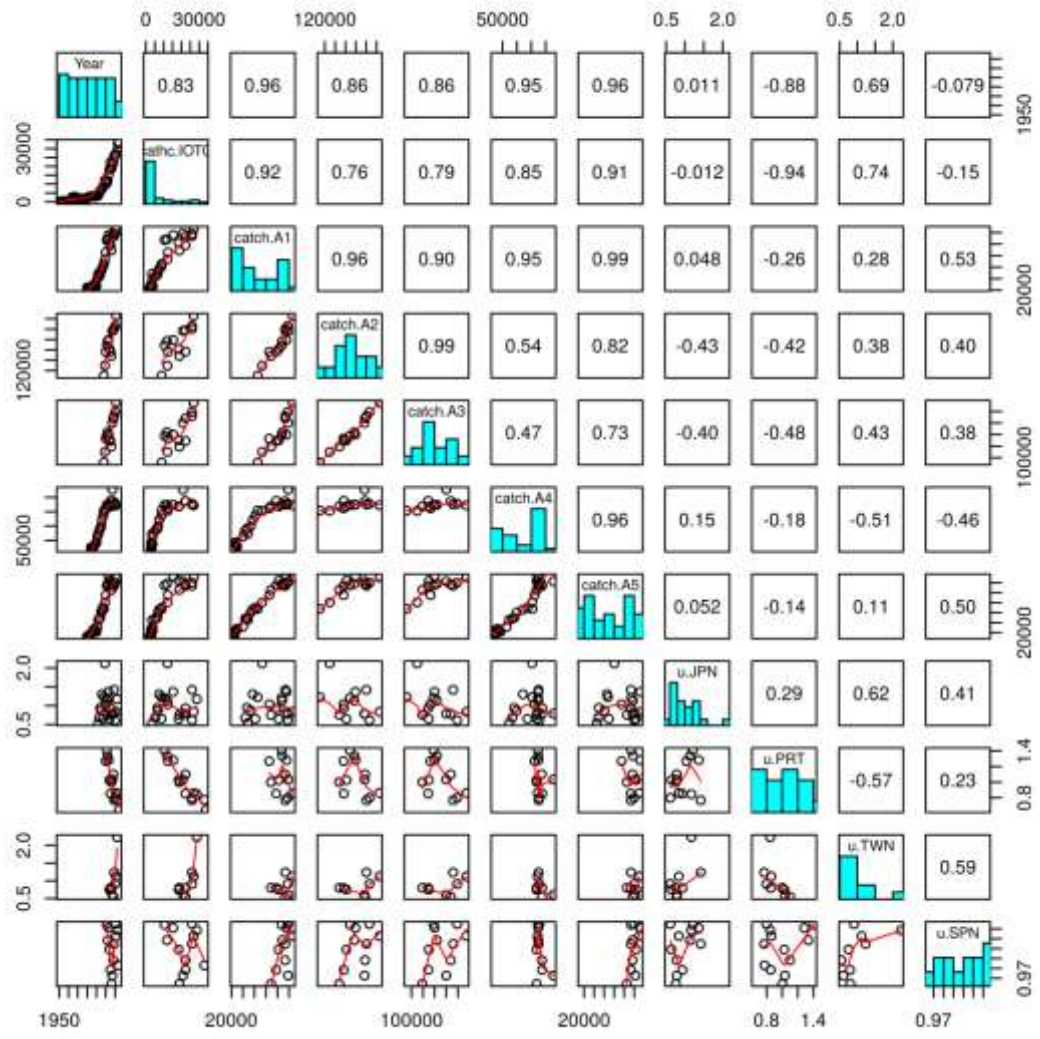

Figure 2 – Estimations of catch (catch.IOTC, catch.A1, catch.A2, catch.A3. catch.A4, catch.A5) and catch rates of Japan (u.JPN), Portugal (u.PRT), Taiwan (u.TWN) and Spain (u.SPN) used in the analyses.

Convergence and autocorrelations

In the sensitive analyses there are two sets of priors (non-informative and informative) and two catch time series (IOTC and A1). The alternative catch estimations A1 and A2 are longer than the others, but the A1 was selected on subjective ground. The code can be easily adapted to fit the models to other series if further sensitivity analyzes are requested. All the calculations of 97.5% quantile of PSRF (Gelman and Rubin, 1992) were below 1.01 hence all the models have converged if we relay in that criterion. In addition the autocorrelation analyzes indicates a fairly acceptable mixing degree of the samples of the posterior distribution (Appendix I).

Fittings

Fittings of the models to the IOTC catch time series and to the four catch rates using non-informative and informative priors are showed in Figures 3 and 4 respectively, while the fittings to the alternative estimation of catch with non-informative and informative priors are showed in Figures 5 and 6 respectively. State-space models are very flexible because there are many parameters (i.e. $r, k, q_1, \dots, q_m, p_1, \dots, p_N, \tau^2, \sigma^2$). However, if the catch rates are conflictive, some

of them may have more influence. Hence, in spite of the flexibility of the model, quality of the fittings may be not that good for the less influential and/or the shorter time series.

Overall all the models fittings (four cases – two priors and two catch time series) were very much similar. The fittings were grossly flat, though there are some bumps. Only Japan time series cover the 1990's hence the Japan data strongly influenced are fittings to data of 1990's. However notice that the Japan dataset is also influential in the end of the time series.

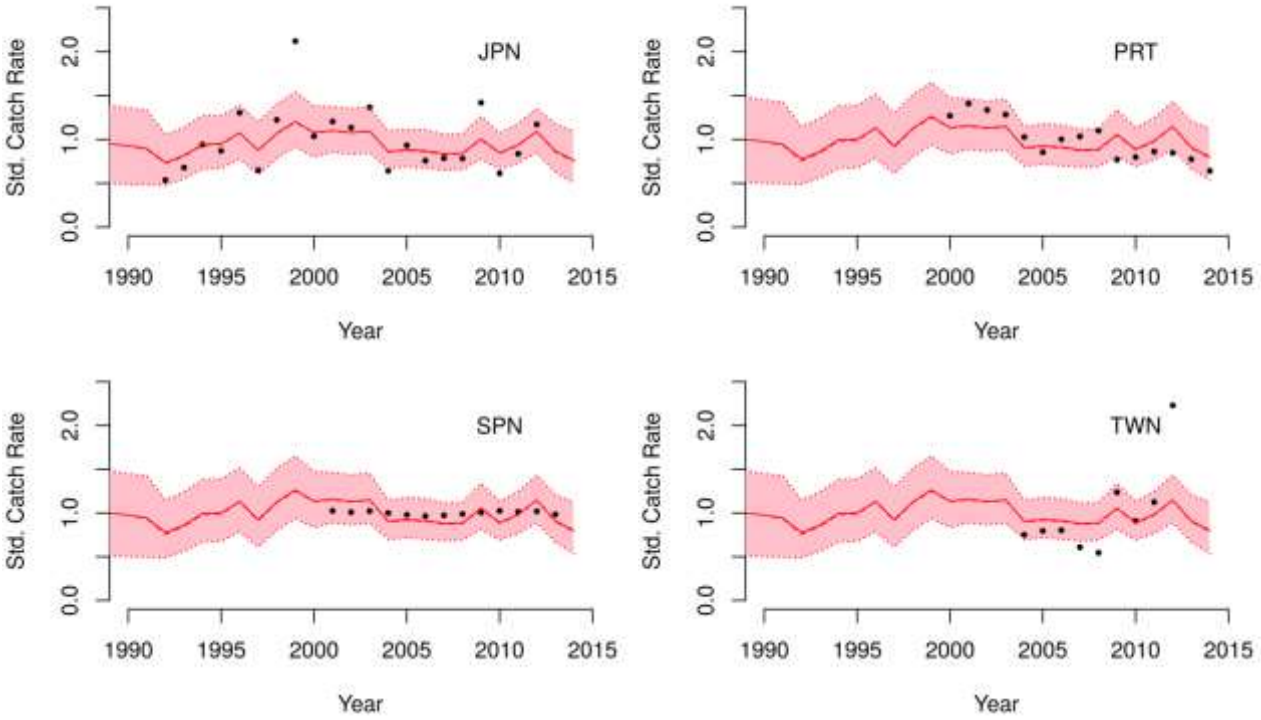

Figure 3 – Model fittings to the estimation of catch as reported in IOTC database and to the four catch time series: Japan (JPN), Portugal (PRT), Spain (SPN) and Taiwan (TWN) as calculated using non-informative prior.

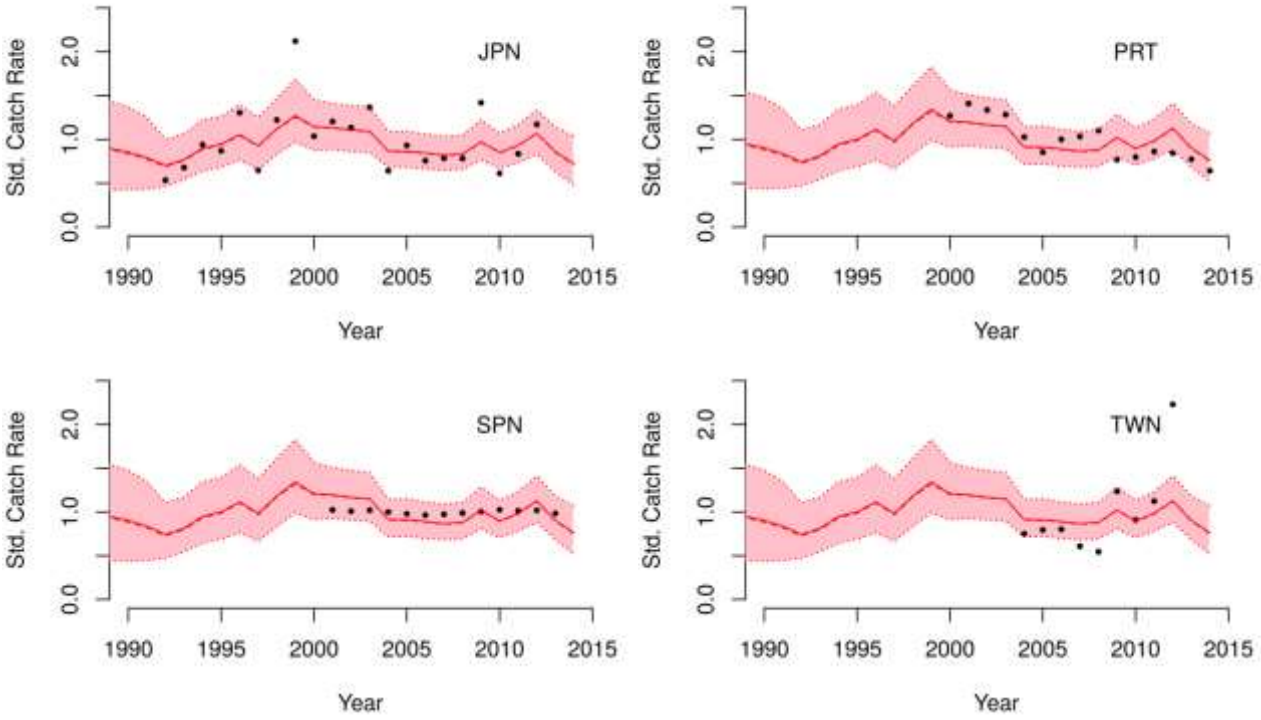

Figure 4 – Model fittings to the estimation of catch as reported in IOTC database and to the four catch time series: Japan (JPN), Portugal (PRT), Spain (SPN) and Taiwan (TWN) as calculated using informative prior.

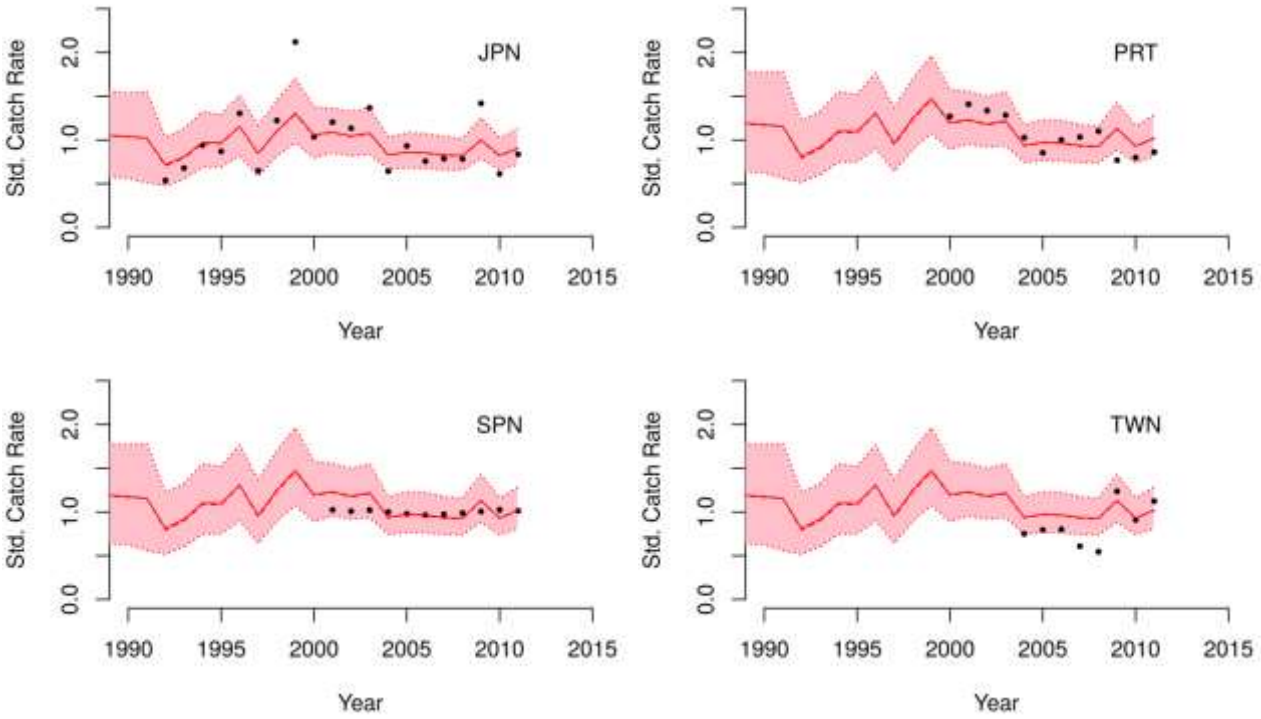

Figure 5 – Model fittings to the alternative estimation of catch and to the four catch time series: Japan (JPN), Portugal (PRT), Spain (SPN) and Taiwan (TWN) as calculated using non-informative prior.

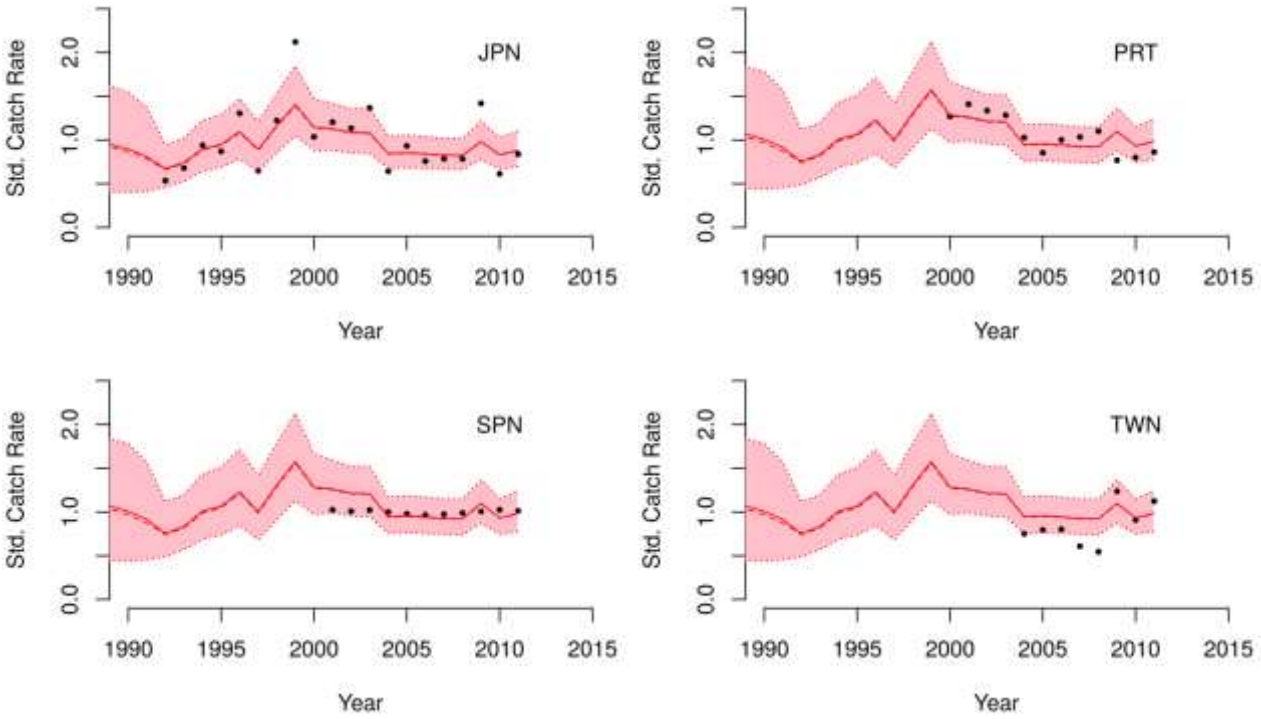

Figure 6 – Model fittings to the alternative estimation of catch and to the four catch time series: Japan (JPN), Portugal (PRT), Spain (SPN) and Taiwan (TWN) as calculated using informative prior.

Residuals

Because the fittings of the four models were all very much similar, only the residuals of one of them (non-informative prior and IOTC catch series) are showed to not clutter (Figure 7). Estimations of the loess model fitted to Japan database indicate the residuals are distributed around a constant close to zero all across the years. Notice that the confidence intervals include the horizontal line close to zero all over the years. This is an indicator that bias is not of concern in the case of the Japan database. However, the outstanding residual of 1999 calls attention.

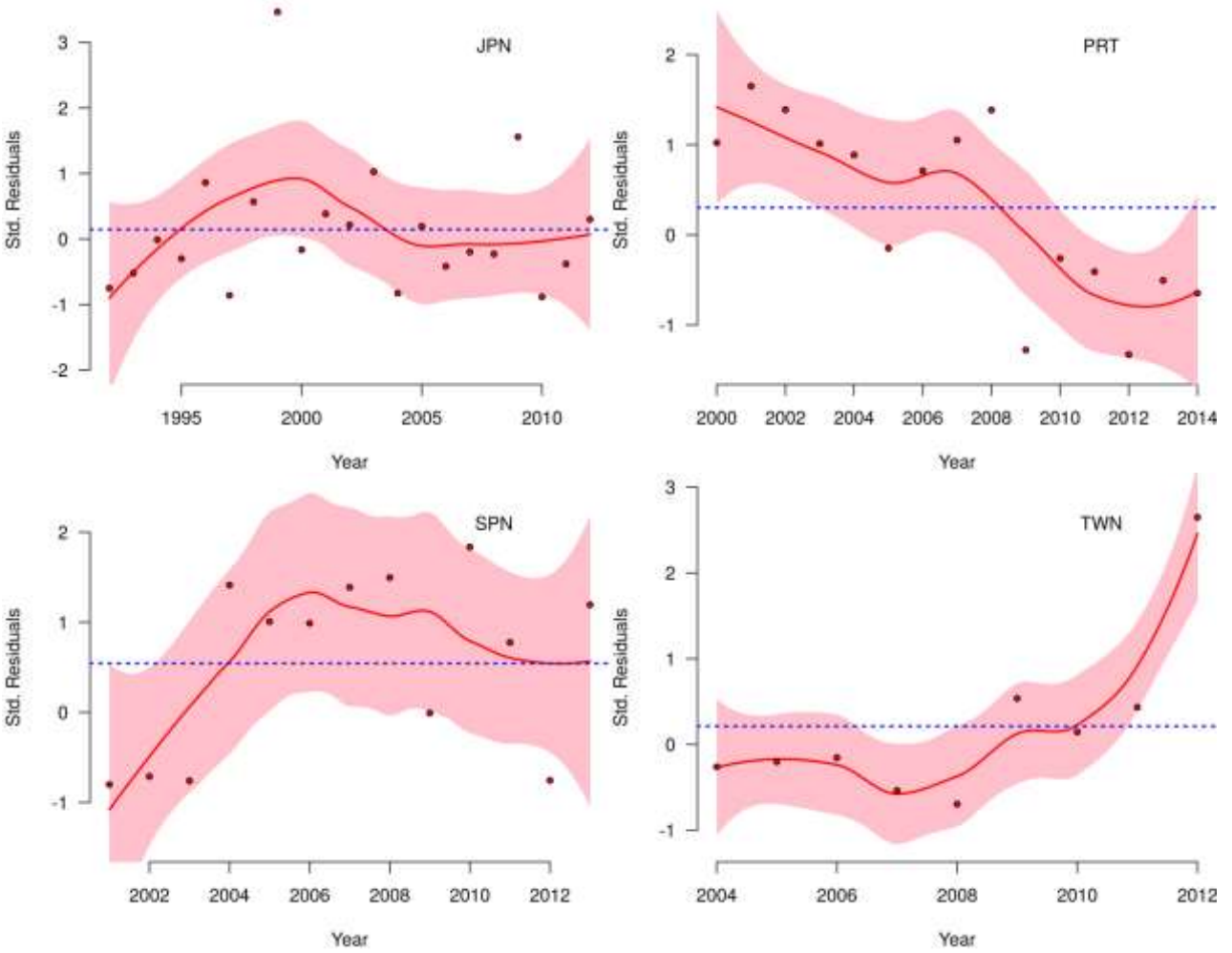

Figure 7 – Standardized residulas of the models fitted to Japan (JPN), Portugal (PRT), Spain (SPN) and Taiwan (TWN) catch rates as calculated based on the estimations of catches as reported in the IOTC databases. Loess models were fitted to the residuals. Polygons filled pink stand for the 95% confidence intervals, while the red lines stand for the punctual estimations. Dotted blue line stands for the mean of the residuals.

Residuals of the models fitted to the Spain, Taiwan and Portugal indicate the models is biases, particularly concerning the later two datasets. Overall residuals of the model fitted to Taiwan catch estimations of 2000's were negative, but they were positive in end of the time series. Further, the very high positive residual of 2012 is of concern. In opposition most of the residuals of the model fitted to Portugal databases were negative in the end of times series. In addition residuals fitted to the beginning of the time series were positive. Overall the loess model fitted to residuals (observed minus predicted) of Portugal indicates that the model is very much biased. Time trends of residuals and of catch rates of Portugal are very much the same. This indicates that the influence of Portugal time series is low. The same applies to Taiwan time series.

Posteriors of parameters

Posteriors calculated for the proportions ($P_t = B_t/k$) were not showed to not clutter. Posteriors of the parameters of interest as calculated based in the four catch rates time series and in the catch estimation as reported in the IOTC databases are showed in Figure 8. Notice that the composite catch rate indices (JPN-PRT-SPN-TWN) do not convey much information concerning the parameters r and k as indicated by the flat posteriors calculated using the non-informative prior. In opposition precision of the posteriors of q, τ^2 and σ^2 were fairly high when the non-informative priors are used in the calculations.

Because the data do not convey much information about the key parameters, the informative priors influences were high on the estimations of k, and particularly r (Figure 8). Notice that the posterior of r as calculated using informative prior was very much similar to the prior density distribution. Posteriors of k were bounded at 700,000 t. However the posterior calculated using the informative prior showed a mode close to 300,000 t. Posteriors of q of the four fleets were similar because the scaled catch rates (values were divided by the mean) were used in the calculations and because the years covered by the four fleets overlaps. Data convey information on the process errors and observational errors. Precisions of the posteriors of observation error (τ^2) as indicated by the narrow density distribution. The inferior limit of posteriors of process errors seems slightly bounded by the prior

.

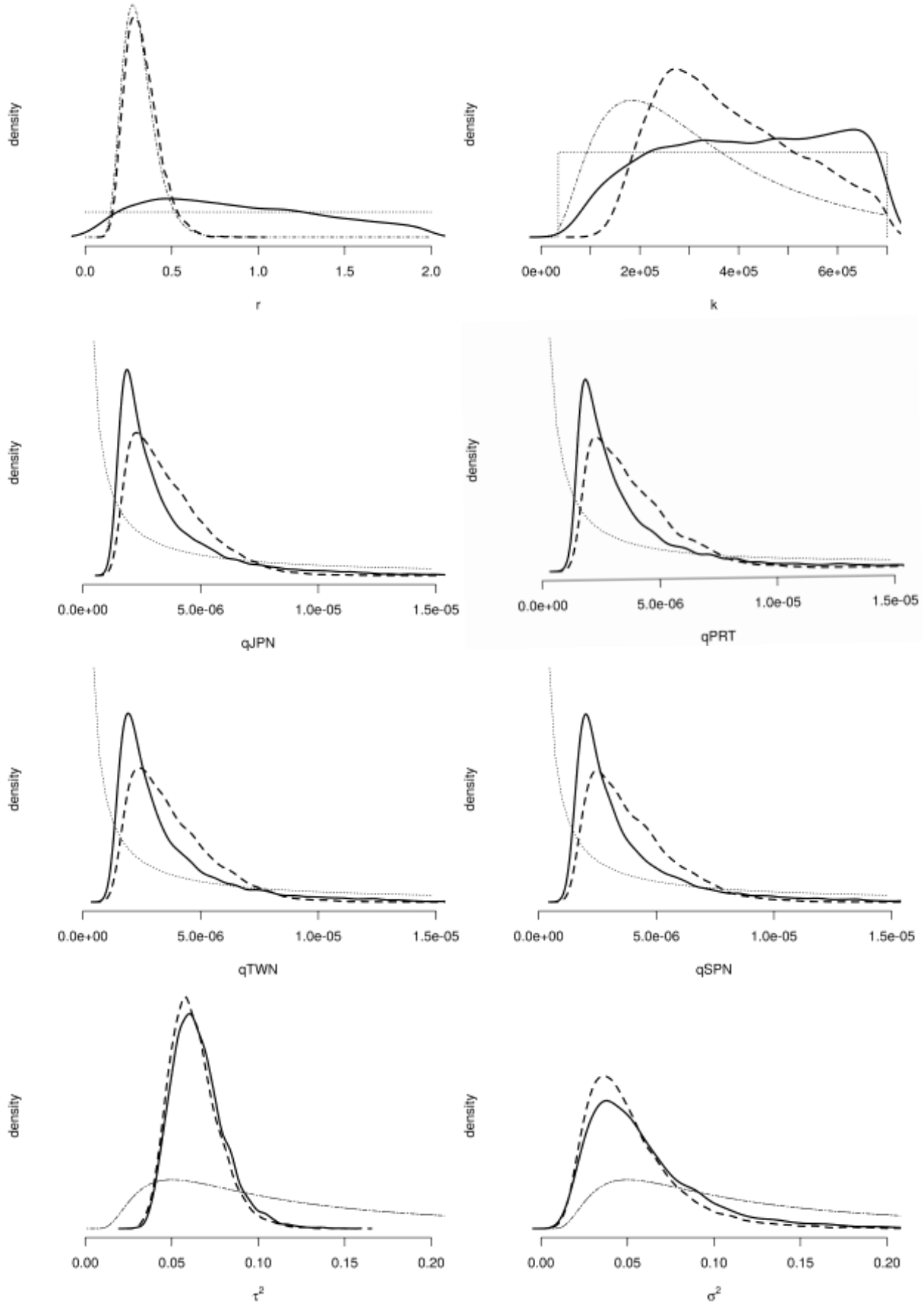

Figure 8 – Posteriors of parameters calculated based on the catch estimations as reported in the IOTC dataset. Thin dotted lines stand for non informative prior. Thin alternating dashed and dotted lines stand for the informative prior. Thick solid lines stand for posteriors calculated using non informative prior. Thick dashed line stands for the posteriors calculated using informative prior.

Posteriors of parameters as calculated based on the alternative estimations of catch are in Figure 9. Overall posteriors of q, τ^2 and σ^2 calculated based on IOTC and on alternative catch estimation give weights to similar values of possible parameters (Figures 8 and 9). However major differences between calculations arise in posteriors of k and r. Posteriors of r calculated based on alternative estimation of catch shifted to right (Figure 9) if compared to posteriors calculated based on the estimations of catch as reported in IOTC databases (Figure 8). Likewise in the calculations based on IOTC catch estimations, the posterior of r calculated using the alternative estimation of catch with non-informative prior is flat, but it was bounded by the prior at the upper limit. In addition, both posteriors of k calculated using the alternative catch estimations were clearly bounded at the upper limit by the priors truncation at 700,000 t (Figure 9). In summary, the posteriors estimated using the alternative catches and the available catch rates point for a very productive stock with a very high carrying capacity.

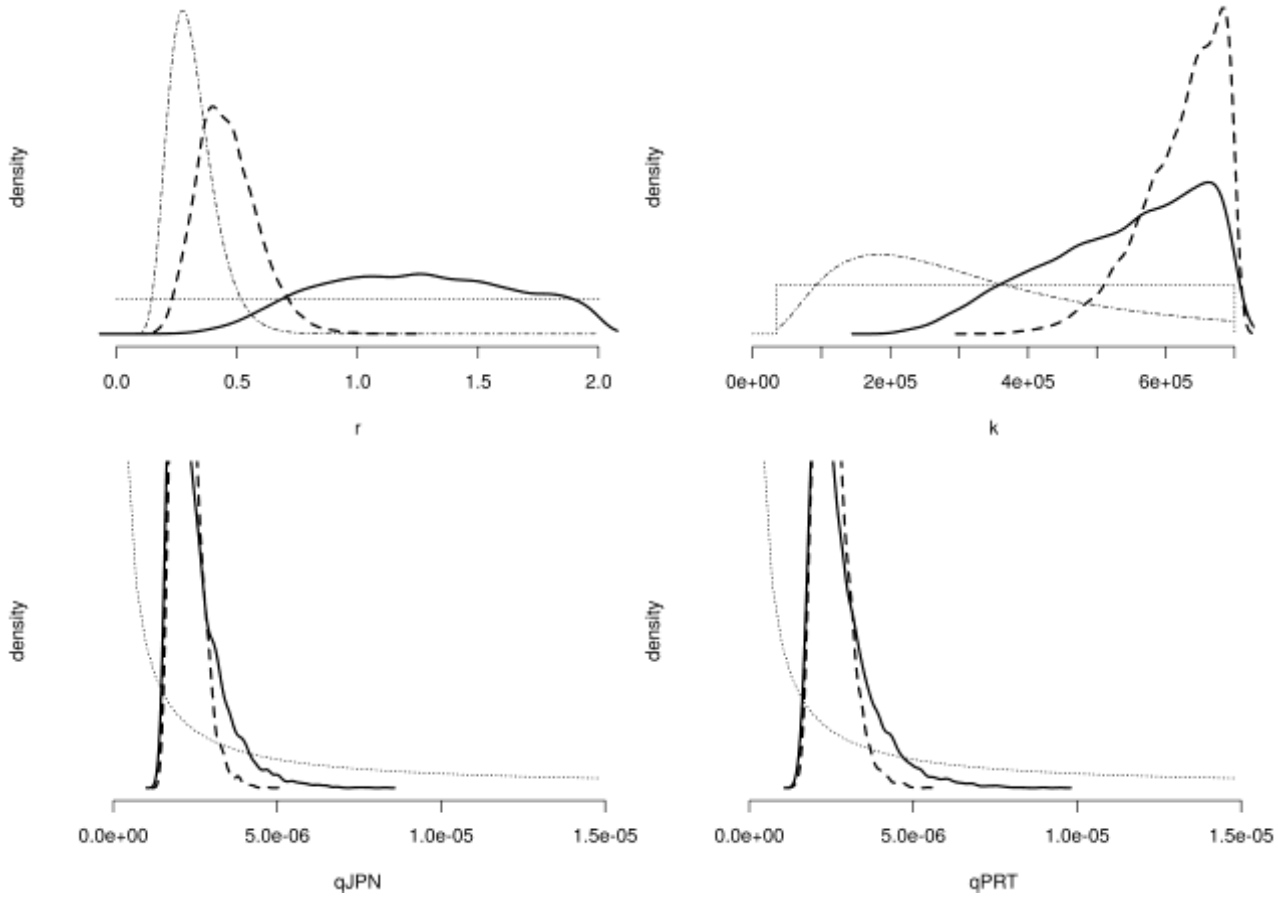

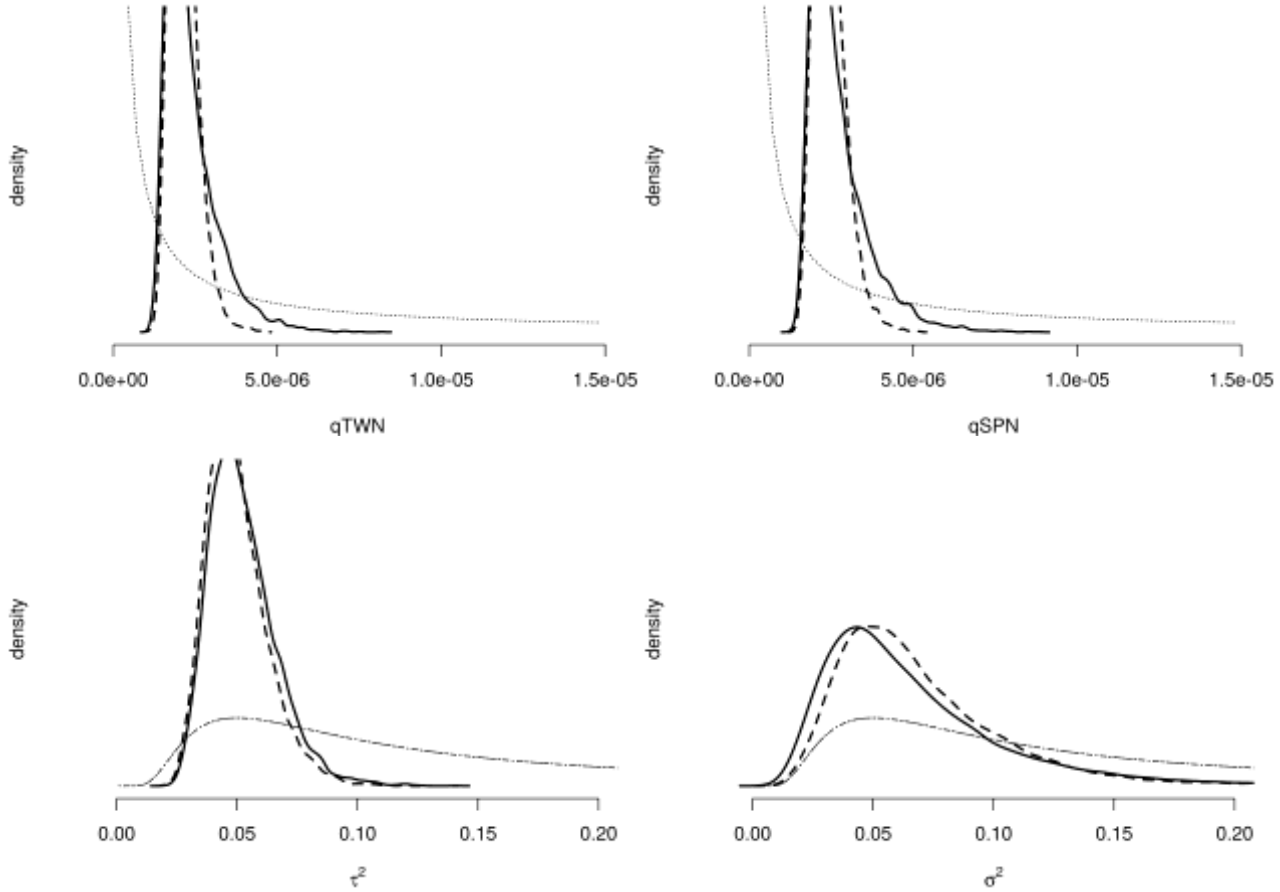

Figure 9 – Posteriors of parameters calculated based on the alternative estimation of catch. Thin dotted lines stand for non informative prior. Thin alternating dashed and dotted lines stand for the informative prior. Thick solid lines stand for posteriors calculated using non informative prior. Thick dashed line stands for the posteriors calculated using informative prior.

Posteriors of benchmarks

Posteriors calculated with non-informative prior based on the estimations of catches reported in IOTC databases were grossly flat, though the posterior of Y_{MSY} gives more weight to values close to 40,000 t. Posterior of Y_{MSY} calculated with informative prior was fairly precise and it gives weight to values between 20,000 and 40,000 t. Posterior of B_{MSY} was wide and it was bounded in the upper limit even when the informative prior was used in the calculations. Even though, one mode appear between 100,000-220,000 t. Precision of harvest rate at MSY was high, the mode was close to 0.18.

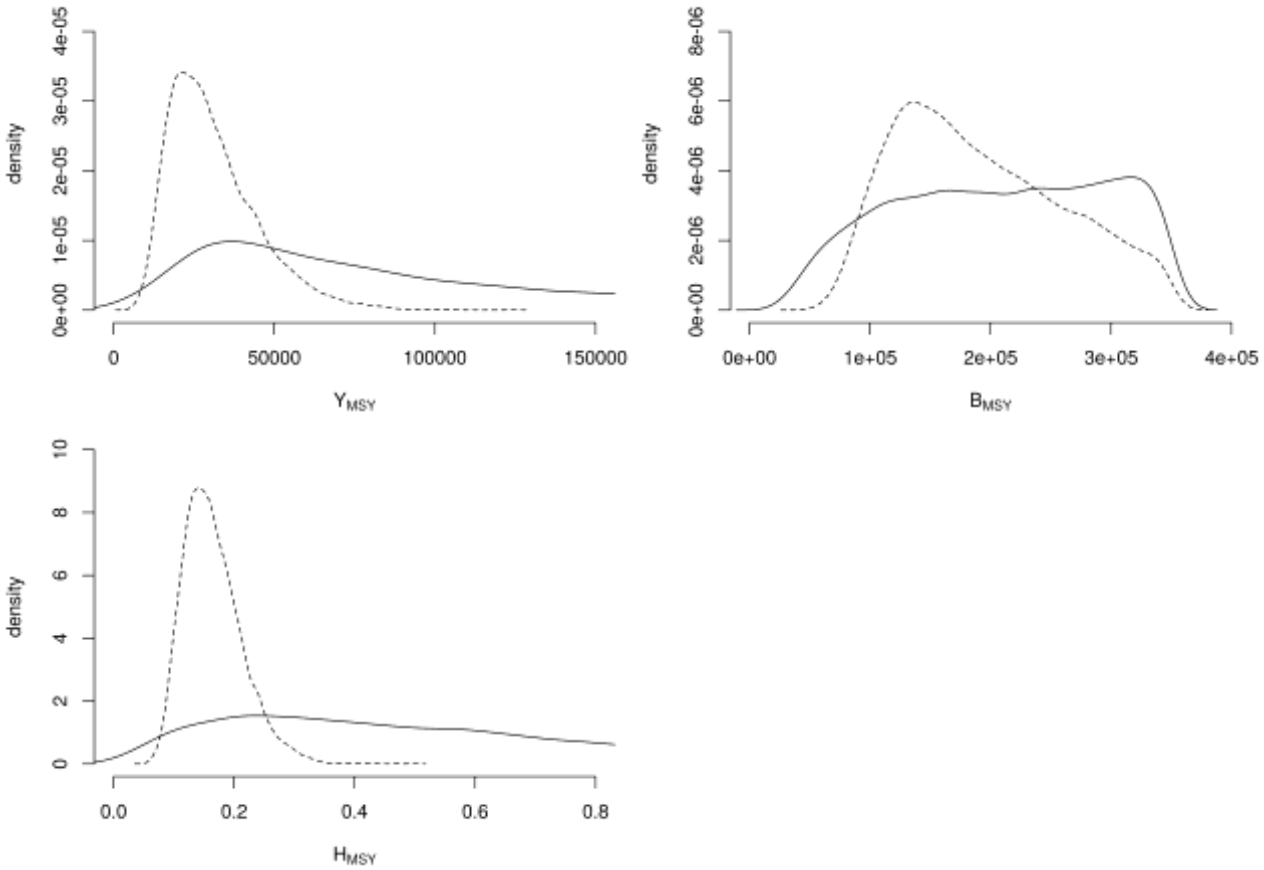

Figure 10 – Posteriors of yield (Y_{MSY}), biomass (B_{MSY}) and harvest (H_{MSY}) at "Maximum Sustainable Yield" calculated based on estimations of catches as reported in the IOTC database. Solid lines stand for the calculations using non-informative prior, while dashed lines stand for posteriors as calculated using informative priors.

Because posteriors of carrying capacity (k) as calculated based on the alternative estimation of catch were all bounded by the upper limit of the priors, posteriors of biomass at MSY ($B_{MSY} = k/2$) were also bounded at the upper limit (Figure 11). Posteriors of yield and of harvest at MSY calculated using non-informative prior were flat and they give weight to very high values. Estimations of posteriors of Y_{MSY} and of H_{MSY} as calculated using informative prior were more precise than those calculated using non-informative priors. Mode of the posterior of Y_{MSY} was close to 70,000 t, while the mode of posterior of H_{MSY} were approximately 0.2.

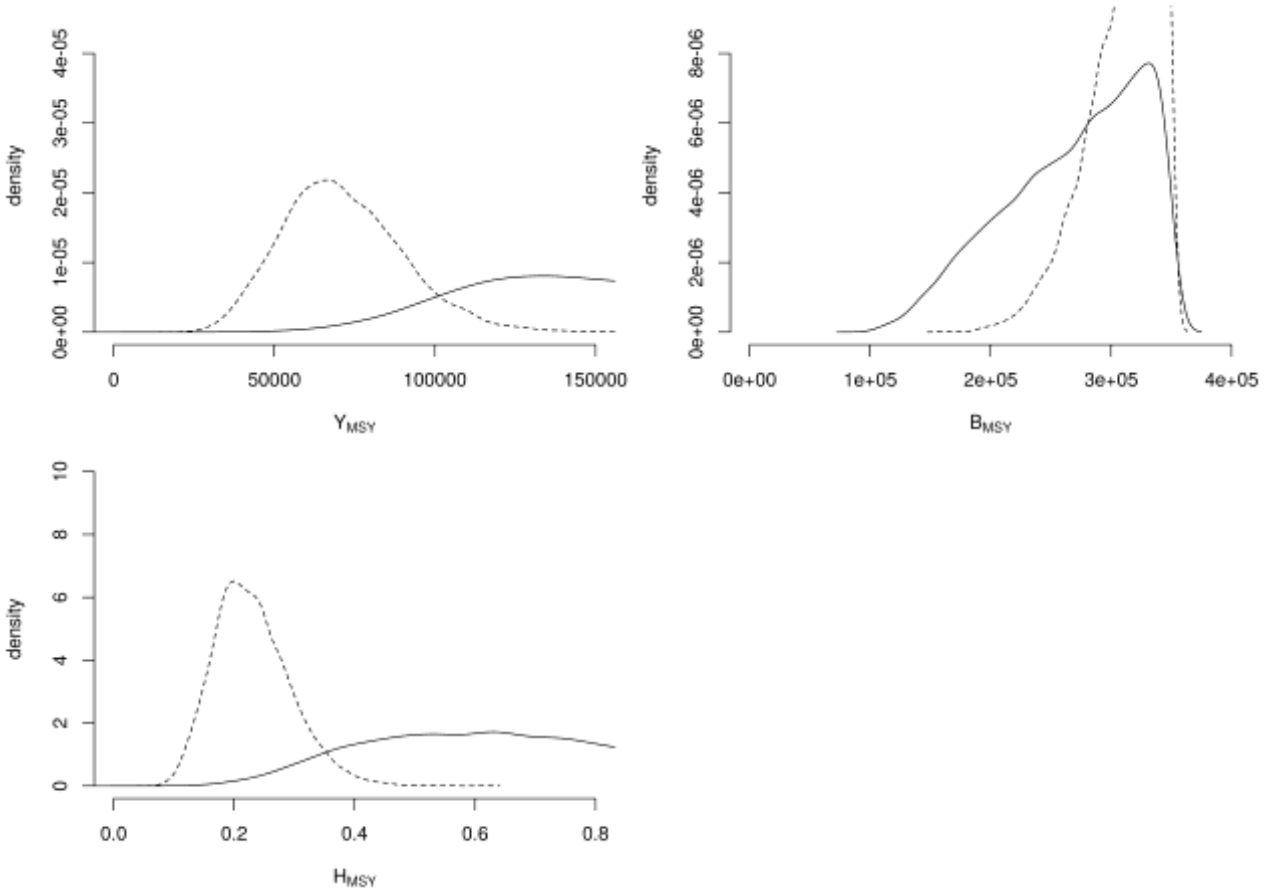

Figure 11 – Posteriors of yield (Y_{MSY}), biomass (B_{MSY}) and harvest (H_{MSY}) at "Maximum Sustainable Yield" calculated based on alternative estimations of catches. Solid lines stand for the calculations using non-informative prior, while dashed lines stand for posteriors as calculated using informative priors.

Joint posteriors and correlations

Contour plots, marginal distributions and correlations of posteriors of parameters and of Y_{MSY} as calculated based on estimations of catches reported in the IOTC databases using non-informative and informative priors are in Figure 12 and Figure 13 respectively. Concerning parameters estimated using non-informative prior (Figure 12) the correlation between k and q call attention. Estimations of Y_{MSY} were correlated to the all model's structural parameters (r, k and q), but the correlation with r was the highest. Contour plots indicate that data conveys little information on the joint distributions of most of the parameters, particularly about those joint distributions in which r or k are considered. Overall joint posteriors of parameters calculated based on informative priors (Figure 13) showed correlations lower correlations than those calculated using non-informative priors (Figure 13). In addition the correlation between the Y_{MSY} and k was higher than the correlation between Y_{MSY} and r.

Calculations of joint posterior distributions based on alternative estimation of catches using non-informative or informative priors are shown in Figures 14 and 15 respectively. Overall pattern showed in contourplots calculated for the alternative estimation of catch were similar to those calculate based on the IOTC catch. However, notice that the correlation between Y_{MSY} and r was very strong when the informative prior was used. This result indicates that the prior of r drives the Y_{MSY} solution.

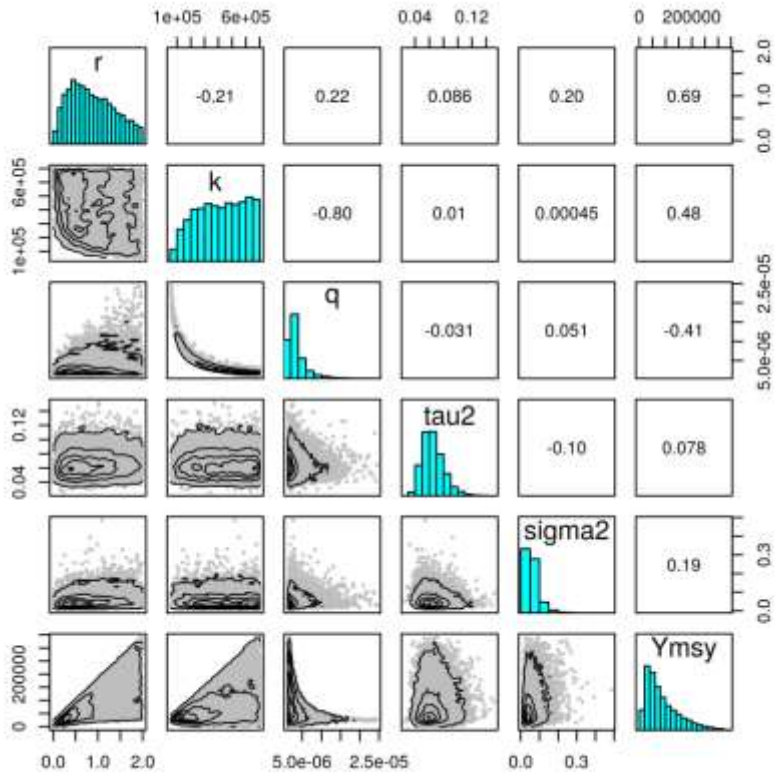

Figure 12 – Marginal and joint posterior distributions of parameters and of yield at MSY as calculated using non-informative prior and catch estimations as reported in the IOTC database.

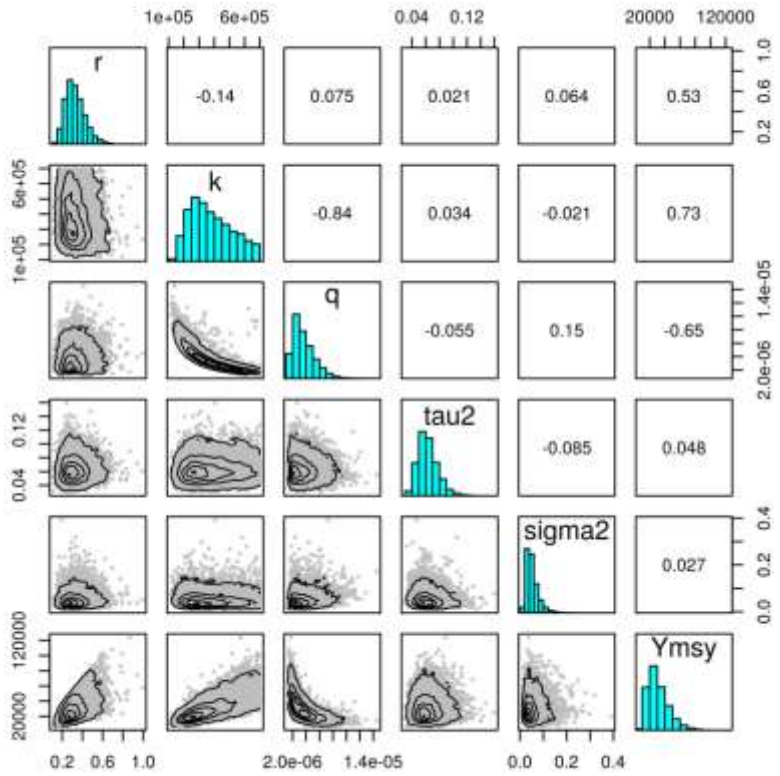

Figure 13 – Marginal and joint posterior distributions of parameters and of yield at MSY as calculated using non-informative prior and the alternative estimation of catch.

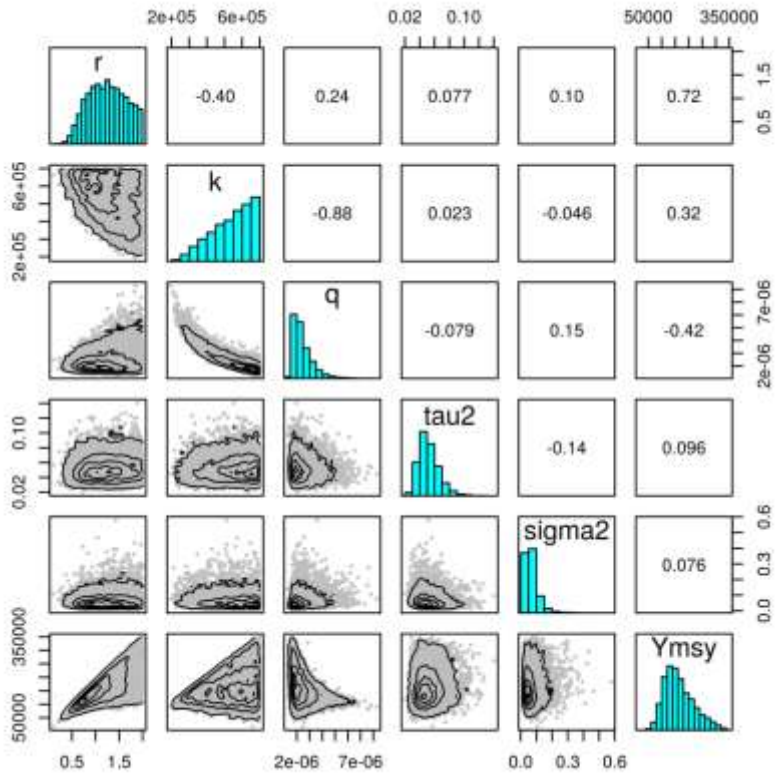

Figure 14 – Marginal and joint posterior distributions of parameters and of yield at MSY as calculated using non-informative prior and alternative estimation of catch.

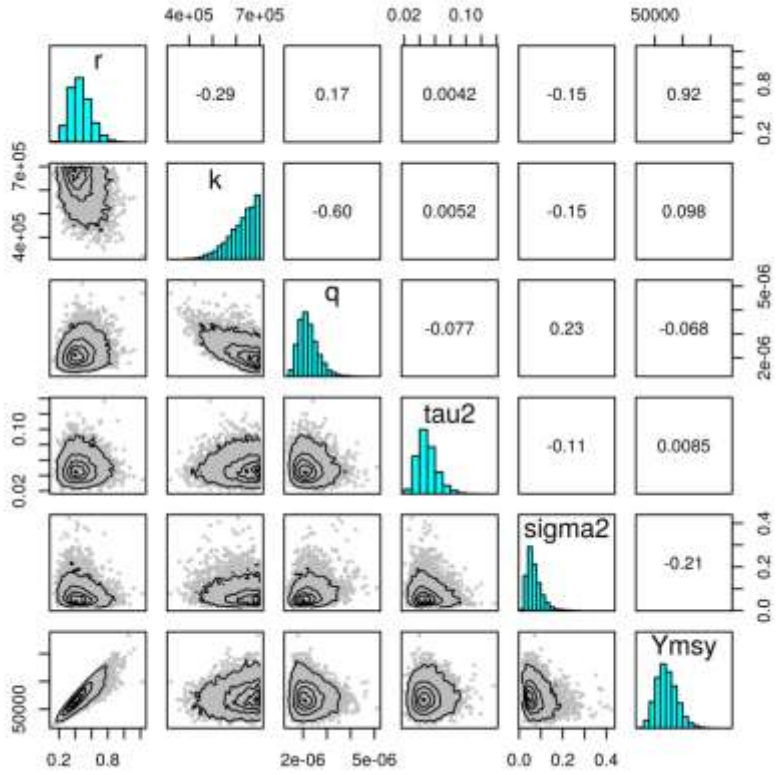

Figure 15 – Marginal and joint posterior distributions of parameters and of yield at MSY as calculated using informative prior and alternative estimation of catch.

Time trends of ratios between harvests in each year and harvest at MSY (H/H_{MSY}), and between biomass in each year and biomass at MSY (B/B_{MSY}), as calculated based on estimations of catches of IOTC are showed in Figure 16. Notice that time trend of estimations of B/B_{MSy} do not show clear time trends. However, the ratio H/H_{MSY} had increased since 2000. In addition, punctual estimations of H/H_{MSY} as calculated using informative prior almost had surpassed 1 in the very end of the time series. Notice that uncertain is high, particularly concerning estimations of H/H_{MSY} after 2002, and that the posterior distributions of H/H_{MSY} showed heavy tail towards high values in the end of the time series.

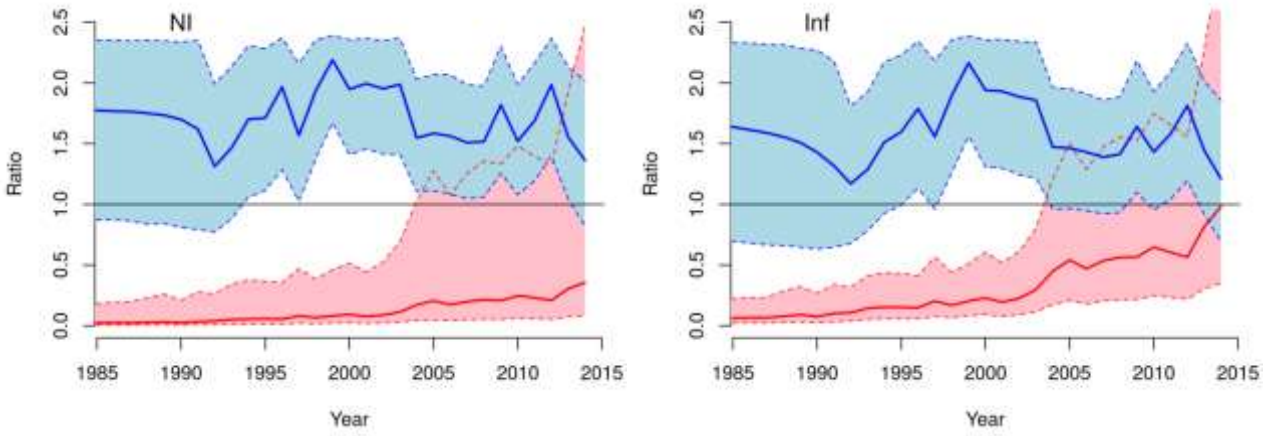

Figure 16 – Ratio between harvest in each year and harvest at MSY (B/B_{MSY}) (bluish colors) and between biomass and biomass at MSY (H/H_{MSY}) (reddish colors). Shaded polygons and dotted lines stand for the credibility intervals, while thick solid lines stand for the medians. Calculations based on non-informative priors are in the left panel (NI), while results gathered with informative prior are in the right panel (Inf).

Posteriors of H/H_{MSY} and of B/B_{MSY} as calculated based on alternative estimation of catches are showed in Figure 17. Credibility intervals of calculations using non-informative prior were wide. Time series of B/B_{MSY} as calculated using non-informative or informative prior showed some up and downs. Notice that estimations of B/B_{MSY} had increased in 1990's, peaked in 2000, and decreased fast until 2004. After 2005 there was not a clear time trend. The ratio H/H_{MSY} had increased all across the years, but faster in the beginning of 2000's. Uncertain concerning estimations of H/H_{MSY} were high, and the posteriors were not symmetric in the end of the time series. Calculations using informative prior indicates that the harvest rate had surpassed the H_{MSY} in the beginning of 2000's. The biomass had decreased but probably, it did not drop to below the -B_{MSY}, at least until 2011.

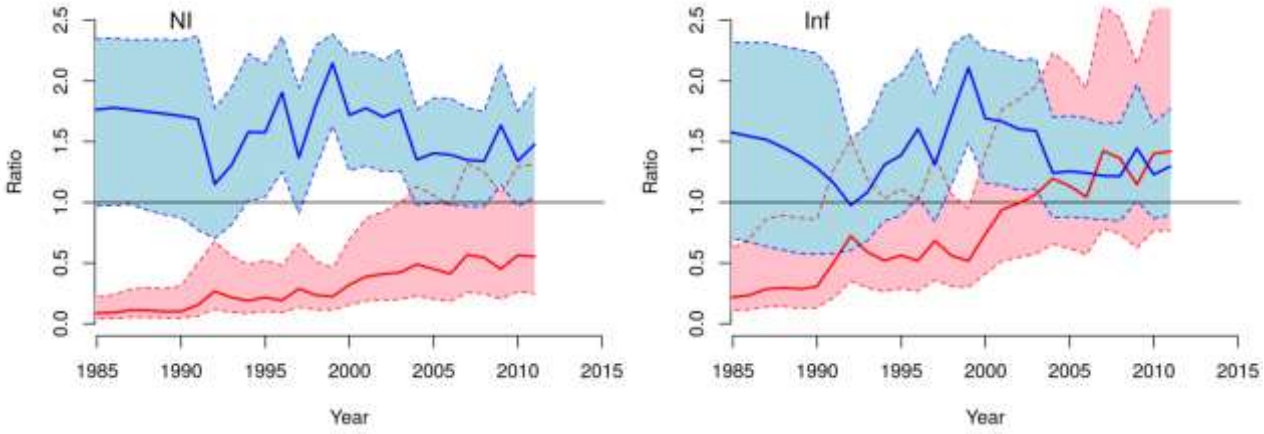

Figure 17 – Ratio between harvest in each year and harvest at MSY (B/B_{MSY}) (bluish colors) and between biomass and biomass at MSY (H/H_{MSY}) (reddish colors). Shaded polygons and dotted lines stand for the credibility intervals, while thick solid lines stand for the medians. Calculations

based on non-informative priors are in the left panel (NI), while results gathered with informative prior are in the right panel (Inf).

Kobe plots calculated based on IOTC estimations of catches are showed in Figure 18, while the calculations based on the alternative estimations of catches are in Figure 19. All the contour plots are wide, hence the uncertain is high. Overall estimations calculated using non informative prior were optimistic in the sense the kernel of the contour plots are in the green are ($B < B_{MSY}$ and $H < H_{MSY}$). In addition, trajectories of marginal medians of H/H_{MSY} and of B/B_{MSY} as calculated using non-informative priors ends up in the green area far from the thresholds $H/H_{MSY} > 1$ and $B/B_{MSY} < 1$. However, estimations calculated using informative prior indicate that ratio H/H_{MSY} is probably higher than 1 as calculated based on alternative estimation of catches. In addition the trajectory of H/H_{MSY} and of B/B_{MSY} ends close to the greed thresholds.

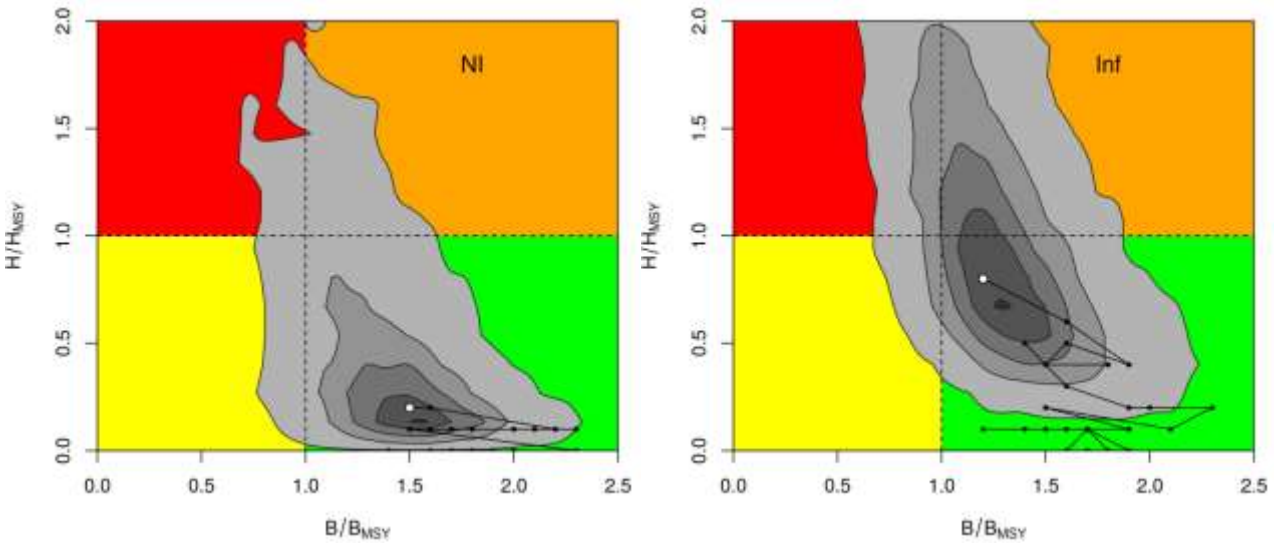

Figure 18 – Contour plotsof posteriors of H/H_{MSY} and B/B_{MSY} calculated based on the IOTC estimations of catches. Solid lines and filled circles stand for the trajectories of marginal medians. NI – non-informative prior; Inf – Informative prior.

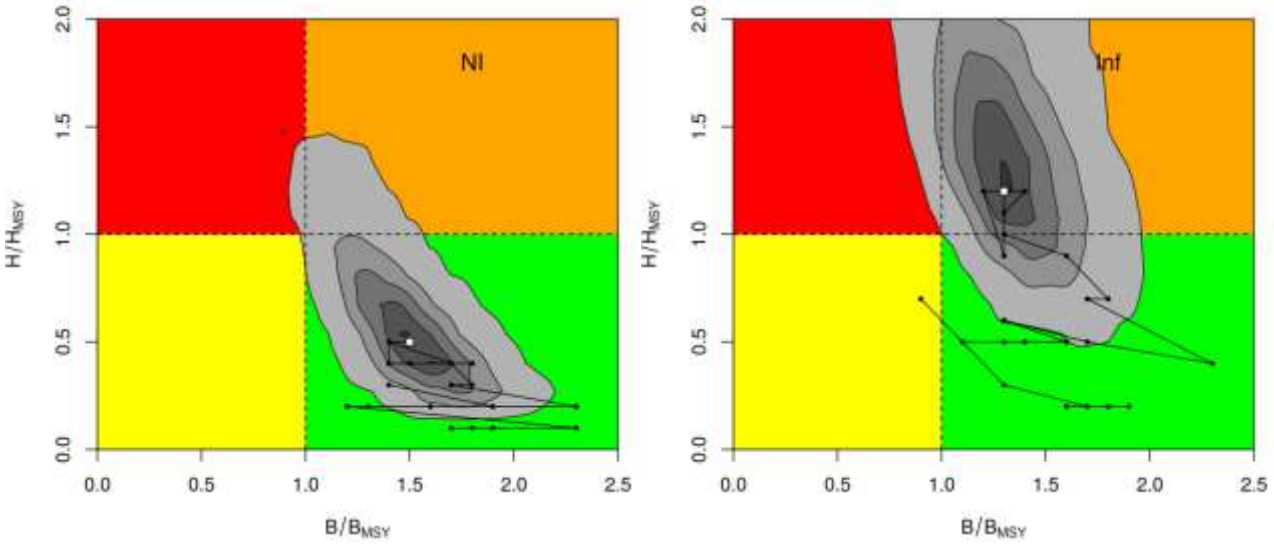

Figure 19 – Contour plotsof posteriors of H/H_{MSY} and B/B_{MSY} calculated based on the alternative estimation of catches. Solid lines and filled circles stand for the trajectories of marginal medians. NI – non-informative prior; Inf – Informative prior.

7. Remarks

Composite indices did not convey much information about key parameters of production models. Time series available for analyses are conflicting. Only Portugal time series are negatively correlated with catch time series. It may worth the effort to analyze separated datasets. Because the composite datasets convey little information about the parameter of the production models the prior distributions were influential when calculating the posteriors. Alternative estimations of catches were much higher than the estimations of catches reported in IOTC databases. Because the alternative catches are high, calculations based on that database have resulted in very high values of k and r. Overall estimations of kobe plots indicate ratio B/B_{MSY} is below 1, but that H/H_{MSY} is above and close to surpass 1.

5. References

Andrade, H. A. 2013. Exploratory stock assessment of the blue marlin (*Makaira mazara*) caught in the Indic Ocean using a State-Space Biomass Dynamic Model. IOTC–2013–WPB11–25.

Andrade, H. A. 2014. Stock assessment of the Indian Ocean swordfish using a Bayesian production model with process and observational errors. IOTC–2014–WPB12–25.

Anon. 2015. Report of the 2015 Iccat blue shark stock assessment session. *manuscript* 115p.

Babcock E.A. and Cortés E. 2015. Bayesian surplus production model applied to blue shark catch, CPUE and effort data. SCRS/2015/150.

Carvalho, F. and Winker, 2015. H. Stock assessment of south Atlantic blue shark (*Prionace glauca*) through 2013. Stock assessment of south Atlantic blue shark (*Prionace glauca*) through 2013. SCRS/2015/153.

Clarke, S. 2015. Historical catch estimate reconstruction for the indian ocean based on shark fin trade data. IOTC–2015–WPEB11–24.

Coelho, R.; Santos, M. N. and Lino, P. G. 2014. Blue shark catches by the Portuguese pelagic longline fleet between 1998-2013 in the Indian Ocean: catch, effort and standardized CPUE. IOTC–2014–WPEB10–24.

Coelho, R.; Lino, P. G.; Rosa, D. and Santos, M. N. 2015. Update of blue shark catches and standardized cpue for the Portuguese pelagic longline fleet in the Indian Ocean: exploring the effects of targeting. IOTC–2015–WPEB11–26.

Denwood, M. J. 2009. runjags: Run Bayesian MCMC Models in the BUGS syntax from within R - manual. http://cran.r-project.org/web/packages/runjags/.

Fernández-Costa, J.; Ramos-Cartelle, A.; García-Cortés, B. and Mejuto, J. 2015. Standardized catch rates for the blue shark (*Prionace glauca*) caught by the Spanish surface longline fleet in the Indian Ocean during the 2001-2013 period. IOTC–2015–WPEB11–25.

Gelman, A. and Rubin, D. B. 1992. A single series from the Gibbs sampler provides a false sense of security. In: Bernardo, J. M., Berger, J. O., Dawid, A. P., Smith, A. F. M. (Eds.). In:Bayesian Statistics, Vol. 4. Oxford University Press, Oxford, pp. 625-631.

IOTC. 2015. Available datasets. <http://www.iotc.org/meetings/11th-working-party-ecosystems-and-bycatch-wpeb11> Accessed: August 17, 2015.

McAllister, M.K., Pikitch, E.K., Punt, A.E., Hilborn, R., 1994. A bayesian approach to stock assessmentand harvest decisions using the sampling/importance resampling algorithm. Can. J. Fish. Aquat. Sci. 51, 2673-2687.

McAllister, M.K., Kirkwood, G.P., 1998. Bayesian stock assessment: a review and example application using the logistic model. ICES J. Mar. Sci. 55: 1031-1060.

Plummer, M., 2005. JAGS: Just Another Gibbs Sampler. Version 1.0.3 manual. http://www-ice.iarc.fr/~martyn/software/jags/.

Plummer, M.; Best, N.; Cowles, K. and Vines, K. 2006. CODA: Convergence diagnosis and output analysisfor MCMC. R News. 6(1), 7-11.

Punt, A.E., Hilborn, R., 1997, Fisheries stock assessment and decision analysis: the Bayesian approach. Rev. Fish Biol. Fish. 7, 35–63.

R Core Team. 2014. R: A Language and Environment for Statistical Computing. R Foundation for Statistical Computing, Vienna, Austria. ISBN 3-900051-07-0, URL http://www.R-project.org/.

Tsai, W-P. and Liu, K-M. 2014. Standardized catch rates of blue sharks caught by the Taiwanese longline fishery in the Indian Ocean. IOTC-2014-WPEB10-25 Rev_1.

APPENDIX I

Autocorrelation analyzes for the four models fitted.

Non-informative prior – Estimations of catches as reported in IOTC databases

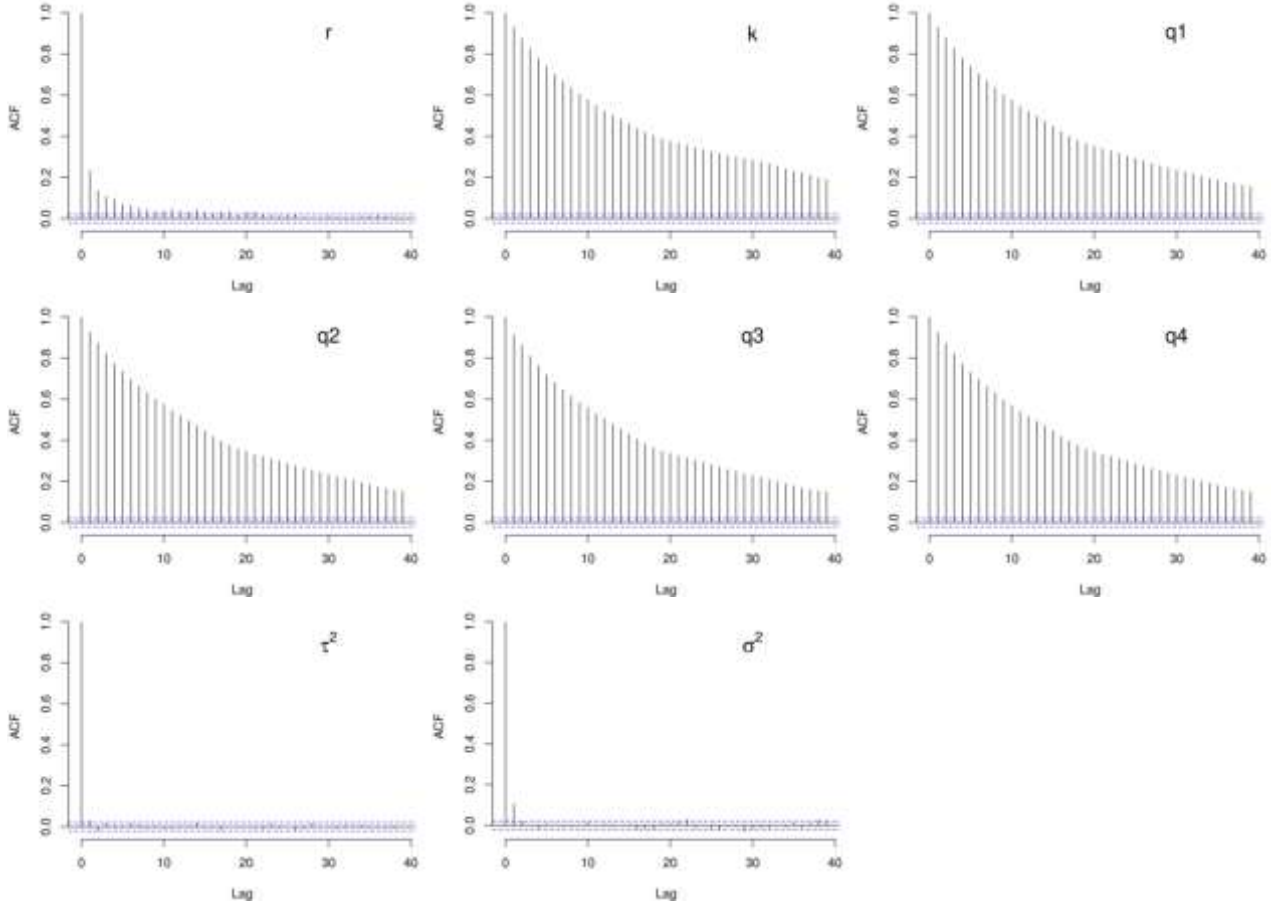

Informative prior – Estimations of catches as reported in IOTC databases

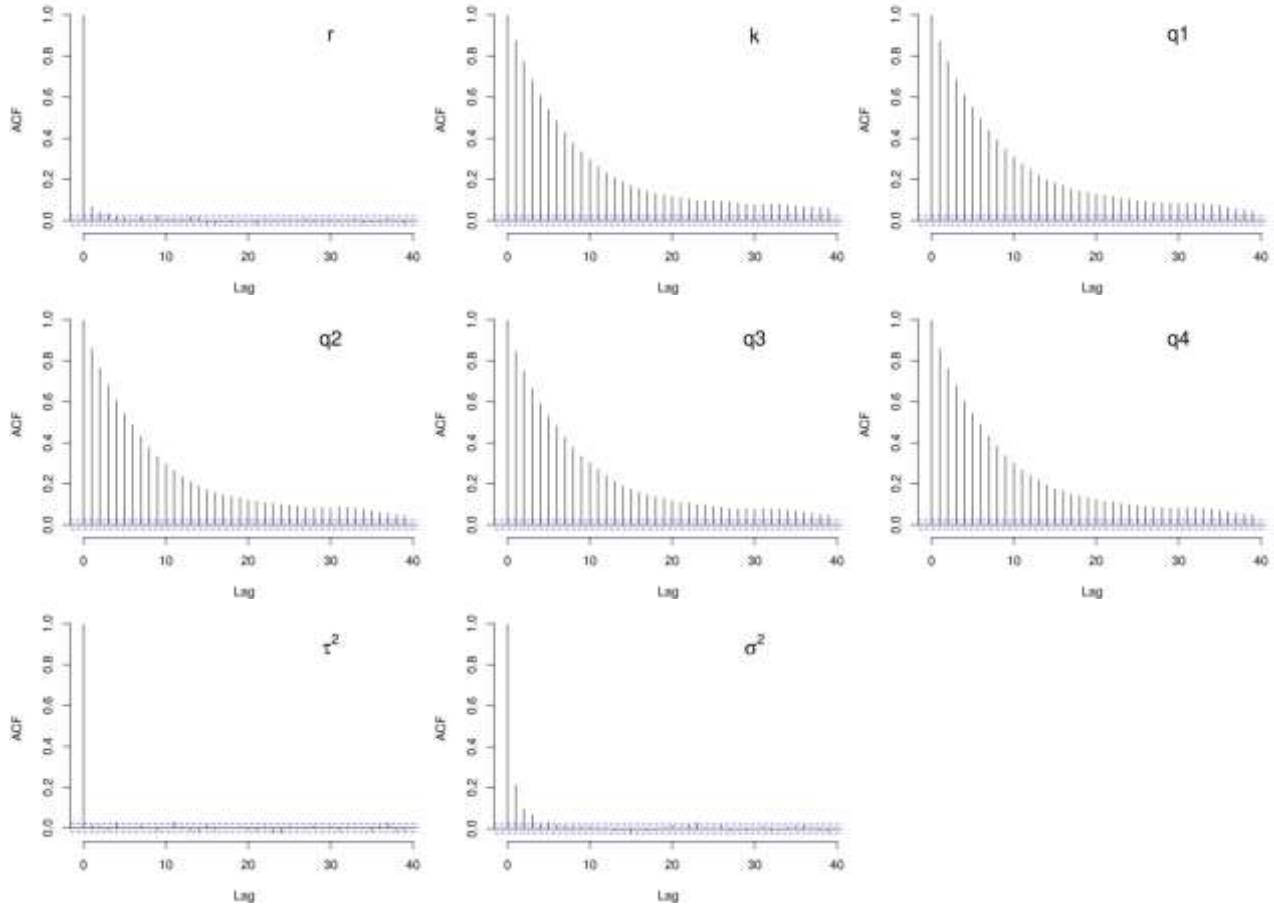

Non-informative prior – Alternative estimation of catches

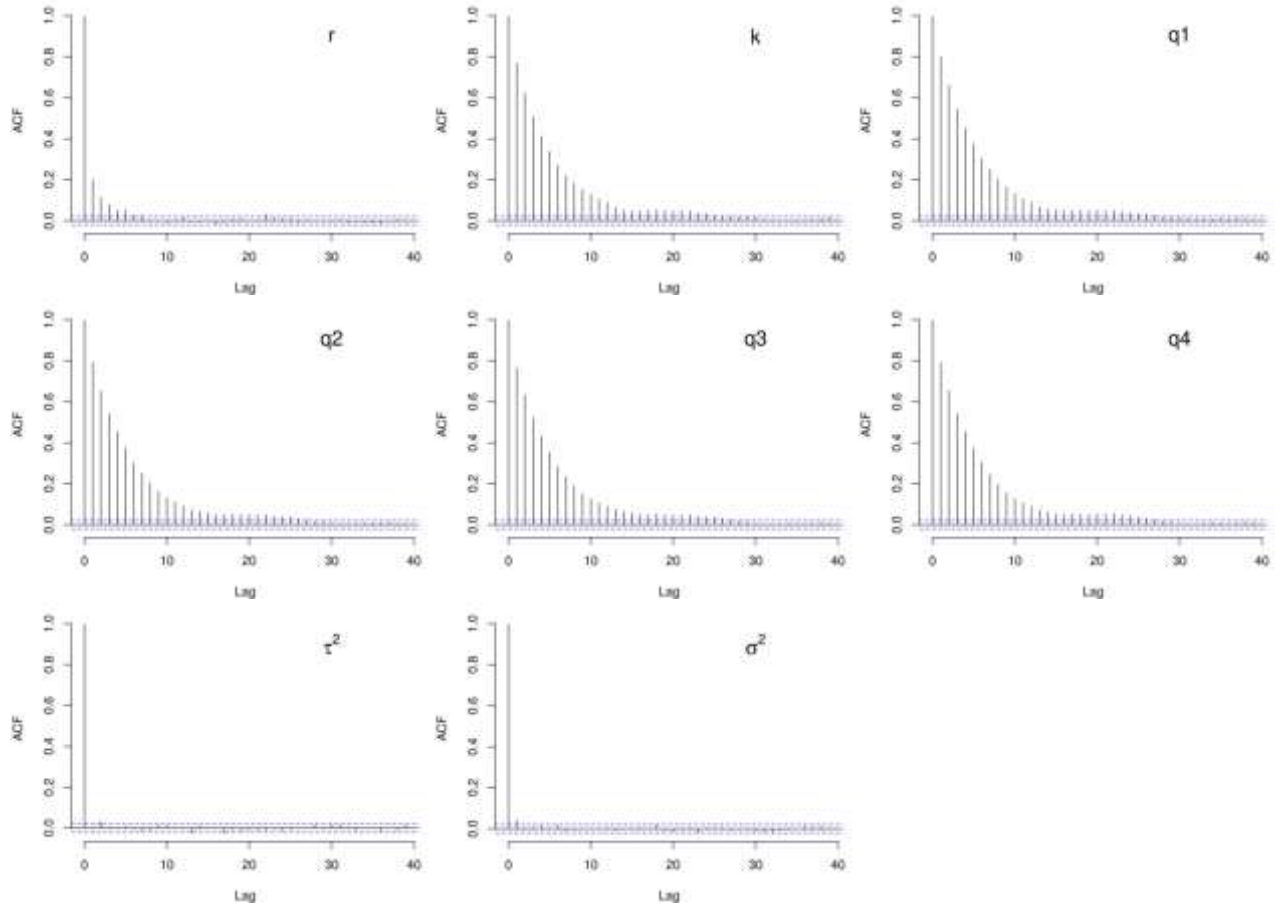

Informative prior – Alternative estimation of catches